

Influence of working medium on the characteristics of two-phase loop thermosyphon under high internal flow resistance

Jingyu Cao ^{1*}, Ling Zheng ¹, Jinqing Peng ¹, Zhanying Zheng ³, Mingke Hu ⁴, Qiliang Wang ⁵, Gang Pei ^{6*}

¹ College of Civil Engineering, Hunan University, Changsha, 410082, China (Corresponding Author)

³ Institute for Turbulence-Noise-Vibration Interaction and Control, Shenzhen Graduate School, Harbin Institute of Technology, Shenzhen 518055, China

⁴ Department of Architecture and Built Environment, University of Nottingham, University Park, Nottingham, NG7 2RD, UK

⁵ Department of Building Services Engineering, The Hong Kong Polytechnic University, Kowloon, Hong Kong, China

⁶ Department of Thermal Science and Energy Engineering, University of Science and Technology of China, Hefei 230027, China (Corresponding Author)

ABSTRACT

Two-phase loop thermosyphon is promising in free cooling of data center, base station, and other industrial buildings with high temperature heat source. The large-scale circulation loop of its natural phase-change cycle is complex with high internal flow resistance in these context and thus is hardly related to the thermodynamic properties of working medium, which has yet to be revealed in detail. In this study, a distributed steady-state model was implemented to verify the heat transfer performance of a two-phase loop thermosyphon with different working mediums under high internal flow resistance for building air-conditioning. Simulative study shows that the behaviors of R744 and R410A are relatively superior, and R744 is outstanding at the extreme high thermal resistance condition. The operating states with different mixed refrigerants are more stable in comparison with pure refrigerants. Eco-friendly mixed refrigerants with low cost and high safety are alternative selections for two-phase loop thermosyphon in building applications.

Keywords: thermosyphon, heat transfer, building cooling, refrigerant

NONMENCLATURE

Abbreviations

Symbols

A	cross section area [m ²]
d	diameter [m]
g	gravitational acceleration [g/m ²]
H	specific enthalpy [J/kg]
h	convective heat transfer coefficient [W/(m ² ·K)]
K	coefficient of regulating valve
L	axial distance along the TPLT [m]
l	axial distance from condenser inlet [m]
M	mass [kg]
M_{mol}	molar mass [g/mol]
m	mass flow rate [kg/s]
P	pressure [kPa]
q	heat flux [W/m ²]
Q	heat exchange capacity [W]
Re	Reynolds number
r	latent heat
T	temperature [K]
x_{th}	thermodynamic quality
<i>Greek letters</i>	
α	void fraction
ξ	flow resistance coefficient
ρ	density [kg/m ³]
μ	dynamic viscosity [kg/(m·s)]
λ	thermal conductive coefficient [W/(m ² ·K)]
ϑ	inclination angle [°]
ε	iterative accuracy

Superscripts

'	liquid
"	vapor

Subscripts

<i>a</i>	accelerated
<i>con</i>	condenser
<i>D</i>	Darcy
<i>d</i>	heat conduction
<i>eva</i>	evaporator
<i>f</i>	frictional
<i>g</i>	ethylene glycol solution
<i>gra</i>	gravitational
<i>H</i>	enthalpy
<i>i</i>	iteration
<i>in</i>	inner
<i>l</i>	local
<i>M</i>	mass
<i>out</i>	outer
<i>P</i>	pressure
<i>s</i>	surface
<i>sat</i>	saturation
<i>t</i>	tube
<i>v</i>	valve
<i>w</i>	water

1. INTRODUCTION

Two-phase loop thermosyphon (TPLT) is widely adopted in thermal management fields as an effective natural two-phase heat transfer device. Its integration into air-conditioner for improving the overall energy efficiency has raised increasingly attention in recent years [1]. However, in a complete free cooling mode, the internal flow resistance of a large-scale loop thermosyphon is high due to its complex pipeline design. Thus, the thermodynamic properties of its working medium have a more significant effect than other system. For example, the loop thermosyphon cooler with R744 is investigated by Zhang et al. [2] for free cooling of data center. Khodabandeh et al. [3] adopted R600a for cooling of radio base station. Chehade et al. [4] conducted simulation in steady operation state of the loop thermosyphon. Their studies are mainly focused on the working medium, structure, and boundary conditions with a relatively low internal flow resistance.

To evaluate the impact of working medium on the heat transfer behavior of a TPLT with high internal flow resistance for its large-scale application in buildings has been designed. In this work, a test rig was built, and the vapor flow resistance could be artificially regulated by a

gate valve. [5] A steady-state distributed parameter model was established, and simulative study on TPLT with various working mediums is conducted. The heat transfer behaviors of the TPLT with 4 mixed refrigerants and 4 pure refrigerants were systematically evaluated.

2. MODEL

2.1 General description

The TPLT includes two-phase and single domains: evaporator, condenser, regulating valve, and liquid and vapour lines (see Fig. 1). It internal refrigerant flow is assisted by the gaps in temperature and altitude, and is regulated by a regulating valve. Detailed structure, operating principle, and geometrical parameters of the TPLT are provided in our previous study [5]. The distributed parameter model is built on following assumptions (parameters vary along axial direction in a 1-D and steady-state domain; and the system is in well insulation) and on the conservations of momentum, energy and mass. Besides, the thermodynamic quality x_{th} is used to indicate the state of the working medium.

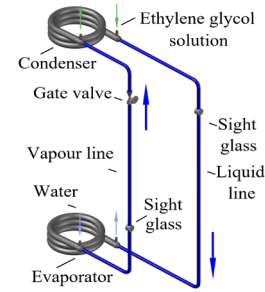


Fig. 1. VCLT diagram

2.2 Momentum calculation

The pressure drops are considered as follows:

Gravitational pressure drop/rise is:

$$dP_{gra} = \rho g dL \sin \theta \quad (1)$$

where the density of working medium in two-phase state is calculated by void fraction.

$$\rho = \alpha \rho'' + (1-\alpha) \rho' \quad (2)$$

$$\alpha = \left[1 + \left(\frac{1-x_{th}}{x_{th}} \right) \frac{\rho''}{\rho'} \right]^{-1} \quad (3)$$

Frictional pressure drop is calculated as:

$$dP_f = \lambda \frac{dL}{d} \frac{m^2}{2\rho A^2} \quad (4)$$

where λ is equal to $64/Re$ for laminar flow and $0.3164/Re^{0.25}$ for turbulent flow, and McAdams correlation is employed for two-phase state:

$$Re = \frac{m}{\pi d} \left(\frac{x_{th}}{\mu''} + \frac{1-x_{th}}{\mu'} \right) \quad (5)$$

The accelerated pressure drop in evaporator is:

$$dP_a = \left(\frac{m}{A}\right)^2 d \left(\frac{(1-x_{th})^2}{\rho'(1-\alpha)} + \frac{x_{th}^2}{\rho''\alpha} \right) \quad (6)$$

Local pressure drop is:

$$dP_l = \xi_l \frac{u^2 \rho}{2} \quad (7)$$

Valve pressure drop is depending on the opening degree,

$$dP_v = K \xi_v \frac{u^2 \rho}{2} \quad (8)$$

where empirical value of K were given by [5].

2.3 Energy calculation

Gnielinski correlation is used for convective heat transfer coefficient of liquid.

$$h = \frac{Nu \lambda}{d} \quad (9)$$

Nu of laminar flow is 4.364 while following equations is adopted for turbulent flow:

$$Nu = \frac{\xi_D (Re - 1000) Pr}{1 + 12.7 \xi_D^{0.5} (Pr^{0.66} - 1)} \quad (10)$$

$$\xi_D = 0.125 (1.82 \log Re - 1.64)^{-2} \quad (11)$$

Dittus-Boelter equation is used for vapor.

$$h = 0.023 Re^{0.8} Pr^{0.4} \frac{\lambda}{d} \quad (12)$$

Semi-empirical equation is adopted for vaporisation.

$$h = 540 Pr^{0.394} q^{0.54} (1 - x_{th})^{-0.65} M_{mol}^{-0.5} \quad (13)$$

Nusselt correlation is applied for condensation. [5]

$$h = 1.13 \left(\frac{\lambda^3 \rho^2 r g}{\mu^2 z (T_{sat} - T_s)} \right)^{0.25} \quad (14)$$

2.4 Algorithm

Figure 2 shows the calculative algorithm, employing REFPROP 9 and MATLAB 2018. Based on the assumed pressure, enthalpy, and mass flow at the inlet of evaporator, the state of next node can be calculated, and the calculation is repeated for all the remaining nodes. When the state of the final node is different from the initial one, the assumed values are regulated for a next

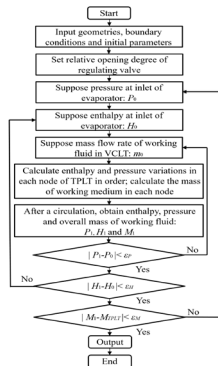


Fig. 2. Computational algorithm [5].

iteration. Finally, when the difference between the pressure, enthalpy and mass are lower than 0.5%, 0.2% and 0.6%, respectively, calculation is complete.

3. RESULTS AND DISCUSSION

3.1 General comparison

Considering the phase-change latent heat, viscosity, and density characteristics as well as environmental features, 4 mixed refrigerants and 4 pure refrigerants are selected for comparison. The filling ratio and boundary conditions remains constant according to the reference [5], whereas the heat source and heat sink temperatures are varied to 300 K and 280 K, respectively. The flow resistance glass 1 to 3 respectively correspond to the opening angle of the gate valve at 90°, 60°, 30°.

Figure 3 compares the heat exchange capacity of TPLT using different refrigerants as responses to the flow resistance glass. The TPLTs with R744, R290, and R401A show relatively high heat exchange capacity under the high flow resistances. The superiority of R744 is extremely obvious when the flow resistance rises to glass 3 as its heat exchange capacity of 138.6 W is more than 50% higher than other refrigerants. Besides, it is observed that the behaviors of R744, R245fa, and R600a remains relatively stable at different flow resistance glass. However, the rest refrigerants show inconsistent performances under different flow resistance glass. For example, the heat exchange capacity of TPLT with R401A ranks fifth, second, and fourth, respectively, as the flow resistance glass changes from 1 to 3.

Figure 4 shows the mass flow rate of TPLT with various refrigerants and flow resistance glasses. Since the latent heat and sensible heat of the 8 refrigerants are different, the relative value of mass flow rate is significantly different from the heat exchange capacity given a flow resistance glass; but the variations versus flow resistance glass are generally similar. The mass flow rate is reduced from 2.31 g/s to 0.72 g/s as the flow resistance glass changes from 1 to 3, while that for R600a only changes within 0.13~0.58 g/s. Generally speaking,

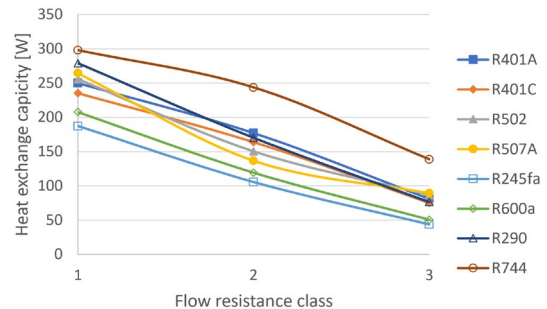


Fig. 3. Heat exchange capacity versus flow resistance class.

the mass flow rate of R401A is relatively moderate at different flow resistance glasses.

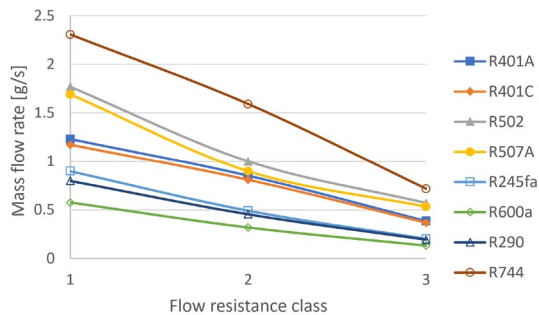


Fig. 4. Mass flow rate versus flow resistance class.

3.2 Characteristic under high flow resistance

To further reveal the behaviors of TPLT under extremely high flow resistance, the flow resistance is set as glass 3, and the internal characteristics are studied as follows. The overheat and undercooling of TPLT with different refrigerants is presented in Fig. 5. The overheat and undercooling of TPLT with R744 is 7.2 K and 2.8 K, respectively, which is the smallest compared with other refrigerants. The overheat and undercooling of TPLT with R401A and R401C is also relatively lower, and its overheat and undercooling is both close to 7.0 K. The one with high overheat normally corresponds to a low heat exchange capacity.

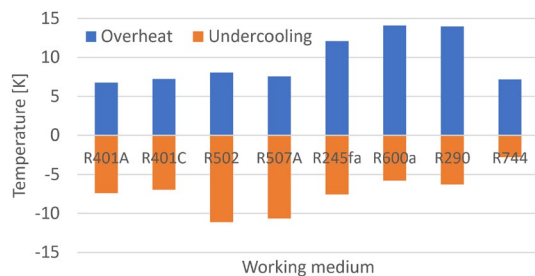


Fig. 5. Overheat and undercooling at flow resistance class 3.

Figure 6 compares the internal and external thermal resistances of TPLT with various refrigerants. It is shown that the internal thermal resistance of TPLT with R744 is only 0.08 K/W whereas that of mixed refrigerants slightly changes within 0.16~0.20 K/W. The ratio of internal thermal resistance to the overall one is 58.7% when the working medium is R744, which is significantly lower

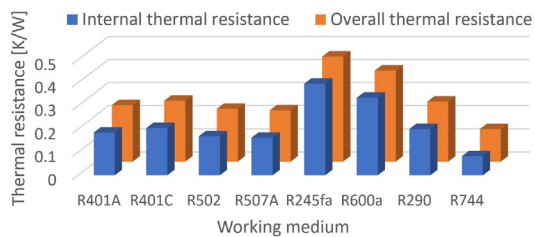


Fig. 6. Thermal resistances at flow resistance class 3.

those for other refrigerants. The influence of high flow resistance to the behavior of R744 is the minimum and is significantly weaker than other pure refrigerant, whereas the mixed refrigerants show similar performance in this adverse condition.

4. CONCLUSIONS

The heat transfer performance of a two-phase loop thermosyphon with different working mediums is evaluated under high internal flow resistance for building air-conditioning. The behaviors of R744 and R410A are relatively superior, and R744 is outstanding at the extreme high thermal resistance condition. The mixed refrigerants show more similar performance in this adverse condition in comparison with pure refrigerants. Results indicate that eco-friendly mixed refrigerants with low cost and high safety are alternative selections in building applications.

ACKNOWLEDGEMENT

The study was sponsored by the National Key Research and Development Project (2018YFB1900602), the Anhui Provincial Natural Science Foundation (2008085QE234), the Fundamental Research Funds for the Central Universities (531118010653), and the Science and Technology Innovation Program of Hunan Province(2020RC5003).

REFERENCE

- [1] Cao J, Zheng Z, Asim M, Hu M, Wang Q, Su Y, Pei G, Leung MKH. A review on independent and integrated/coupled two-phase loop thermosyphons. *Applied Energy* 2020;280:115885.
- [2] Zhang H, Shao S, Tian C. Numerical investigation of a CO₂ loop thermosyphon in an integrated air conditioning system for free cooling of data centers. *Appl Therm Eng* 2017;126:1134–1240.
- [3] Khodabandeh R. Thermal performance of a closed advanced two-phase thermosyphon loop for cooling of radio base stations at different operating conditions. *Appl Therm Eng* 2004;24:2643–2655.
- [4] Chehade A, Louahlia-Gualous H, Masson SL, Lepinasse E. Experimental investigations and modelling of a loop thermosyphon for cooling with zero electrical consumption. *Appl Therm Eng* 2015;87:559–573.
- [5] Cao J, Hong X, Zheng Z, Asim M, Hu M, Wang Q, Pei G, Leung MKH. Performance characteristics of variable conductance loop thermosyphon for energy-efficient building thermal control. *Applied Energy* 2020;275:115337.